Available online at www.sciencedirect.com
SCIENCE DIRECT®
International Journal of Thermal Sciences 42 (2003) 921–930
International Journal of Thermal Sciences
www.elsevier.com/locate/ijts

Reflections on lumped models of unsteady heat conduction in simple bodies

Cristóbal Cortés [a,*], Antonio Campo [b], Inmaculada Arauzo [a]

[a] *Department of Mechanical Engineering, University of Zaragoza, María de Luna 3, 50018 Zaragoza, Spain*
[b] *Department of Mechanical Engineering, The University of Vermont, Burlington, VT 05405, USA*

Received 9 July 2002; accepted 20 December 2002

Abstract

This paper re-examines the venerable lumped model of unsteady heat conduction by means of a detailed study of the exact temperature distributions in bodies of elementary geometry (i.e., large slab, long cylinder and sphere). The space-mean temperature is used as a vehicle for demonstrating that the lumped calculation directly follows as a particular case from the infinite series solution of the general distributed model. In this manner, several methods to find a limit Biot number can be established as simpler alternatives to the traditional procedure. Additionally, the discussion offers a different perspective of this classical subject of heat conduction theory, gaining more insight on the limiting behavior of unsteady temperature distributions.

1. Introduction

Fundamentally, the Biot number, $Bi = hL/k$, constitutes a dimensionless form of the convective coefficient, h, that regulates the heat transmission between the surface of a solid body and a neighboring fluid. This heat exchange process occurs by way of an interplay of two thermal resistances, one due to heat conduction within the body whose thermal conductivity is k, and the other arising from heat convection between the surface and the fluid.

To accept a simplistic lumped model of unsteady heat conduction, the conductive thermal resistance has to be negligible in comparison with the convective thermal resistance, meaning that Bi becomes very small [1,2], i.e.,

$$Bi \ll 1 \implies T \approx T_L(t) \tag{1}$$

where T is the real temperature field and T_L designates its estimation via the lumped assumption. Thereby, this criterion can be satisfied by certain bodies that

(a) are very small in size,
(b) are constructed from materials with large thermal conductivities, or
(c) are exposed to weak convective environments.

From a strict quantitative standpoint, the question is, however, how small Bi should be in order to comply with the above condition.

For bodies of simple geometry (large slab, long cylinder and sphere), the answer has been traditionally deduced from the distributed model of heat conduction [1,2]. When subjected to a convective boundary condition, the analytical temperature solutions of the one-dimensional heat conduction equation consistently reveal that whenever

$$Bi \leqslant 0.1 \tag{2}$$

the ratio of the temperature at the surface to that at the center of the body differs from unity by less than 5%, i.e.,

$$\frac{T(L,t) - T_f}{T(0,t) - T_f} = \frac{T_s(t) - T_f}{T_o(t) - T_f} \geqslant 0.95 \tag{3}$$

The development of this criterion involves a trial-and-error procedure, in which the two extreme local values of T are compared for all times under progressively lower Biot numbers until Eq. (3) is satisfied.

Based on these premises, the following categoric statement arises: The simple lumped model is amenable for situations which are characterized by $Bi \leqslant 0.1$, thus collapsing the entire temperature distribution into a single value without large errors, Eq. (1). In contrast, for $Bi > 0.1$, the lumped model fails, and the general distributed model needs to be applied forcibly in order to compute T.

* Corresponding author.
E-mail address: tdyfqdb@posta.unizar.es (C. Cortés).

1290-0729/$ – see front matter
doi:10.1016/S1290-0729(03)00070-X

Nomenclature

A	convective area
Bi	Biot number, $= hL/k$
c	specific heat
C_n	constants of the series solution
f	eigenfunctions of the series solution
F	space integrals in the series solution of $\bar{\theta}$, Eq. (18)
h	convection coefficient
k	thermal conductivity
L	characteristic length (half-thickness of a slab, radius of a cylinder, radius of a sphere)
s	geometric parameter
t	time
T	temperature
$\overline{T}$	space-mean temperature
V	volume
x	space coordinate (Cartesian, cylindrical radius, spherical radius)

Greek letters

α	thermal diffusivity, $= k/\rho c$
η	dimensionless space coordinate, $= x/L$
θ	dimensionless temperature, $= (T - T_f)/(T_i - T_f)$
$\bar{\theta}$	dimensionless space-mean temperature, $= (\overline{T} - T_f)/(T_i - T_f)$
ρ	density
τ	dimensionless time or Fourier number, $= \alpha t/L^2$
τ^*	dimensionless critical times for the one-term approximation
ξ_n	eigenvalues for the series solution

Subscripts

1	first term of the series, one-term solution
f	fluid
i	initial
L	lumped model
o	center of the one-dimensional body, $\eta = 0$
s	surface of the one-dimensional body, $\eta = 1$
n	general term of the series

Notwithstanding, a salient feature of this line of reasoning should be made apparent. The comparison, as well as its companion error condition, Eq. (3), refer only to the exact temperature distribution. A literature search indicates that a direct scrutiny involving the models themselves, in conjunction with the two temperatures produced by them (T and T_L), has not been reported so far.

This paper seeks to answer the aforesaid question in a convincing manner, linking the variations of temperature with time produced by the two candidate models. To accomplish this objective, the spatial average of T, $\overline{T}$, is considered as the quantity to be compared with T_L. In fact, throughout the derivations and calculations, it is demonstrated that the lumped model is a particular case of the more general distributed model for the space-mean temperature. When the latter is applied to the three simple bodies in question under vanishingly small Biot numbers, the resultant infinite series solution for $\overline{T}$ reduces to a single exponential expression which depends solely on Bi. This expression is finally shown to match the classical, lumped description of unsteady convective cooling.

2. Convective cooling of simple bodies

Fig. 1 illustrates the unsteady cooling of a one-dimensional solid (large slab, long cylinder and sphere) with uniform initial temperature, $T = T_i$, thoroughly. At $t = 0$, the body surface is suddenly exposed to a convective environment which is characterized by a uniform heat transfer coefficient, h, and a constant fluid temperature, T_f. The thermophysical properties of the material are not influenced by temperature.

An adequate set of dimensionless variables for this problem is

$$\theta = \frac{T - T_f}{T_i - T_f}, \qquad \eta = \frac{x}{L}, \qquad \tau = \frac{\alpha t}{L^2}, \qquad Bi = \frac{hL}{k} \tag{4}$$

where $T_i - T_f$, L and L^2/α are the scales adopted for the temperature T, the coordinate x and the time t, respectively. The dimensionless time, τ, is also frequently designated as the Fourier number. The Biot number, Bi, emerges as a controlling parameter. In accordance with these definitions, the distributed model of the physical situation described above can be compactly formulated as follows:

Heat conduction equation:

$$\frac{\partial\theta}{\partial\tau} = \frac{1}{\eta^{s-1}}\frac{\partial}{\partial\eta}\left(\eta^{s-1}\frac{\partial\theta}{\partial\eta}\right) \tag{5a}$$

Initial condition:

$$\theta(\eta, 0) = 1 \tag{5b}$$

Boundary conditions:

$$\frac{\partial\theta}{\partial\eta}(0, \tau) = 0 \tag{5c}$$

$$\frac{\partial\theta}{\partial\eta}(1, \tau) = -Bi\,\theta(1, \tau) \tag{5d}$$

In Eq. (5a), the geometric parameter s identifies the appropriate coordinate system: $s = 1, 2, 3$ for Cartesian, cylindrical and spherical, respectively.

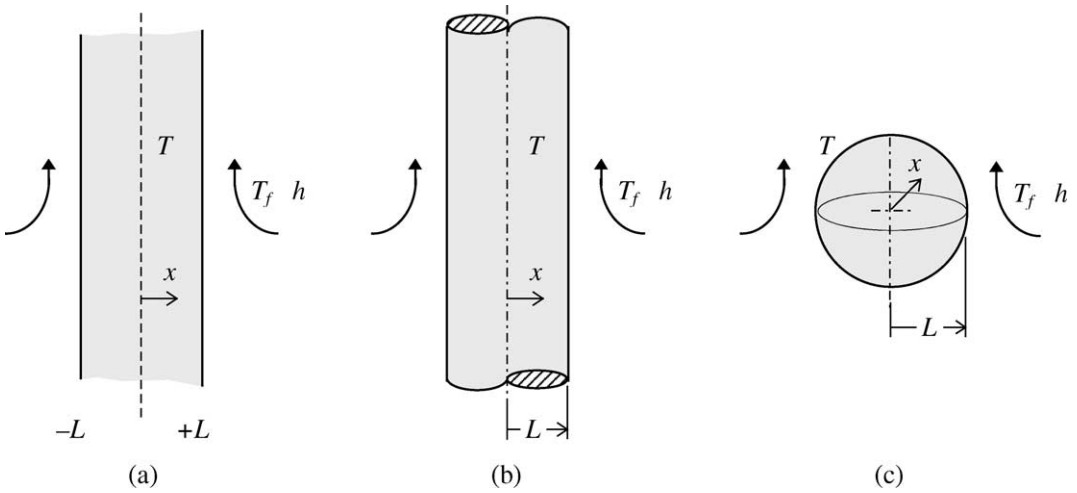

Fig. 1. Unsteady cooling of elementary one-dimensional solids. (a) Symmetrical large plate. (b) Long cylinder. (c) Sphere.

Table 1
Eigenvalues, eigenfunctions and constants of the series solution, Eq. (6)

Geometry	Eigenvalues ξ_n	Constants C_n	Eigenfunctions $f(a)$
Large plate	$\xi_n \sin\xi_n - Bi\cos\xi_n = 0$	$\frac{2\sin\xi_n}{\xi_n+\sin\xi_n\cos\xi_n}$	$\cos a$
Long cylinder	$\xi_n J_1(\xi_n) - Bi\, J_0(\xi_n) = 0$	$\frac{2J_1(\xi_n)}{\xi_n(J_o^2(\xi_n)+J_1^2(\xi_n))}$	$J_0(a)$
Sphere	$\xi_n\cos\xi_n + (Bi-1)\sin\xi_n = 0$	$\frac{2(\sin\xi_n-\xi_n\cos\xi_n)}{\xi_n-\sin\xi_n\cos\xi_n}$	$\frac{\sin a}{a}$

The exact dimensionless temperature distributions, $\theta(\eta,\tau)$, for each of the three basic geometries may be obtained by applying the method of separation of variables to Eqs. (5), to yield the summation of an infinite series:

$$\theta(\eta,\tau) = \sum_{n=1}^{\infty} C_n f(\xi_n\eta)\exp\left(-\xi_n^2\tau\right) \tag{6}$$

The corresponding eigenvalues ξ_n, eigenfunctions f and constants C_n have been summarized in Table 1 [1,2].

3. Lumped model of unsteady conduction

Whenever some restrictions are met, the same situation can be also described by a far more simple lumped model. The classical derivation starts by assuming the temperature field T adequately represented by a uniform value, which we will designate as T_L. Then, an overall energy balance is applied to the body at an arbitrary time t:

$$\rho cV\frac{\mathrm{d}T_L}{\mathrm{d}t} = -hA(T_L - T_f) \tag{7a}$$

which, along with the initial condition

$$T_L(0) = T_i \tag{7b}$$

can be easily integrated to give

$$\frac{T_L(t)-T_f}{T_i-T_f} = \exp\left(-\frac{hA}{\rho cV}t\right) \tag{8}$$

It is interesting to notice that a characteristic time does clearly appear in Eq. (8), given by the quotient $\rho cV/hA$. Consequently, this time scale differs from the one employed previously in the distributed model, i.e., L^2/α. On the other hand, the influence of geometry reduces to the volume-to-area ratio, V/A, to which the meaning of a characteristic length is usually attributed. In this manner, the length scale for our three simple bodies would be also different: L, $L/2$ or $L/3$, depending on whether a large plate, a long cylinder or a sphere is being studied, respectively.

In spite of these considerations, Eqs. (7), (8) can be cast in a coherent nondimensional form by using the previous definitions of θ,τ and Bi in Eq. (4). To this end, it is also necessary to reinterpret the parameter s, noting that the equality $V/A = L/s$ holds for the three elementary geometries. Hence, Eqs. (7), (8) become

$$\frac{\mathrm{d}\theta_L}{\mathrm{d}\tau} = -s\,Bi\,\theta_L(\tau) \tag{9a}$$

$$\theta_L(0) = 1 \tag{9b}$$

$$\theta_L(\tau) = \exp(-s\,Bi\,\tau) \tag{10}$$

4. The concept of a space-mean temperature

A rigorous comparison between the distributed and lumped models should now directly proceed to examine their independent solutions given by Eqs. (6) and (10). However, any intermediate step that properly eliminates the spatial

dependence of the exact solution would be indeed very convenient. Since $\theta(\eta,\tau)$ is bounded in η, this avenue could consist in adopting its maximum, which arises at the body center, $\theta(0,\tau)=\theta_o(\tau)$, and its minimum, occurring at the surface, $\theta(1,\tau)=\theta_s(\tau)$. But independently of this idea, the space-mean temperature offers more simplicity, and, as we will later demonstrate, more significance to the analysis.

The spatial average of the dimensional temperature T is defined as

$$\overline{T}(t)=\frac{1}{V}\int_V T\,\mathrm{d}V \tag{11}$$

If we particularize the analysis to the one-dimensional geometries, and use the definitions expressed in Eq. (4), the corresponding nondimensional form reads

$$\bar{\theta}(\tau)=s\int_0^1 \theta\eta^{s-1}\,\mathrm{d}\eta \tag{12}$$

To explore the meaning of this global quantity, we may recall that the heat conduction equation (5a) is merely an energy balance in differential form. Therefore, this character must be retrieved in a global sense by performing an integration with respect to the space variable η. Firstly, Eq. (5a) is rearranged as

$$\eta^{s-1}\frac{\partial\theta}{\partial\tau}=\frac{\partial}{\partial\eta}\left(\eta^{s-1}\frac{\partial\theta}{\partial\eta}\right) \tag{13}$$

Both sides are now integrated with η from 0 to 1, and then multiplied by the parameter s:

$$s\int_0^1 \eta^{s-1}\frac{\partial\theta}{\partial\tau}\,\mathrm{d}\eta=s\int_0^1\frac{\partial}{\partial\eta}\left(\eta^{s-1}\frac{\partial\theta}{\partial\eta}\right)\mathrm{d}\eta \tag{14}$$

The left-hand side is reordered to permit the differentiation with τ to occur first by virtue of the Leibnitz theorem [3], whereas the right-hand side can be integrated immediately:

$$\frac{\mathrm{d}}{\mathrm{d}\tau}\left(s\int_0^1\eta^{s-1}\theta\,\mathrm{d}\eta\right)=s\left[\eta^{s-1}\frac{\partial\theta}{\partial\eta}\right]_{\eta=1}-s\left[\eta^{s-1}\frac{\partial\theta}{\partial\eta}\right]_{\eta=0} \tag{15}$$

The term varying with time is recognized as the dimensionless space-mean temperature $\bar{\theta}$, Eq. (12). Invoking the boundary conditions, Eqs. (5c) and (5d), the second term on the right-hand side vanishes identically and the first term simply becomes $-s\,Bi\,\theta(1,\tau)$. Therefore, the conversion procedure ends up with the following equation:

$$\frac{\mathrm{d}\bar{\theta}}{\mathrm{d}\tau}=-s\,Bi\,\theta_s(\tau) \tag{16a}$$

to which an initial condition can be attached, as easily deduced from Eqs. (5b) and (12):

$$\bar{\theta}(0)=1 \tag{16b}$$

Table 2
Functions $F(\xi_n)$ for the series solution of the space-mean temperature $\bar{\theta}$, Eq. (17)

Geometry	$F(\xi_n)$
Large plate	$\frac{\sin\xi_n}{\xi_n}$
Long cylinder	$\frac{2J_1(\xi_n)}{\xi_n}$
Sphere	$\frac{3(\sin\xi_n-\xi_n\cos\xi_n)}{\xi_n^3}$

The correspondence between these expressions and the lumped model equations (9) is apparent. From a mathematical standpoint, it can be said that a problem involving a partial differential equation in two independent variables (space η and time τ) having the temperature θ as the dependent variable, Eq. (5a), has been gradually reduced to a first order, ordinary differential equation for the spatial average temperature $\bar{\theta}(\tau)$, Eq. (16a).

However, some information must have been lost due to the integration process. The consequence is that the right-hand side of Eq. (16a) is expressed in terms of the surface temperature $\theta_s(\tau)$. Since this quantity is unknown a priori, the degraded Eqs. (16) cannot be used to obtain an exact solution, although they may constitute the starting point for the implementation of approximate methods of the integral type (see, for instance, [4]).

In order to calculate $\bar{\theta}$, the series solution, Eq. (6), is introduced into Eq. (12), arriving at

$$\bar{\theta}(\tau)=\sum_{n=1}^{\infty}C_n F(\xi_n)\exp\left(-\xi_n^2\tau\right) \tag{17}$$

where $F(\xi_n)$ is a shorthand notation for the integral

$$F(\xi_n)=s\int_0^1 f(\xi_n\eta)\eta^{s-1}\,\mathrm{d}\eta \tag{18}$$

which is explicitly given in Table 2 for the three coordinate systems.

Incidentally, one should note that identical results can be obtained by particularizing Eq. (6) to $\eta=1$, substituting $\theta_s(\tau)=\theta(1,\tau)$ in the global balance, Eq. (16a), and then integrating it under the initial condition.

5. Lumped approximation of the space-mean temperature

In any case, the preceding derivation sheds more light into the meaning of a lumped model. When the η-dependence of the temperature distribution θ is weak, $\theta(\eta,\tau)\approx\bar{\theta}(\tau)$, and, in particular, $\theta(1,\tau)=\theta_s(\tau)\approx\bar{\theta}(\tau)$. Substituting this approximation in Eq. (16a), we retrieve Eq. (9a), so that the differential problems stated by Eqs. (9) and (16) are now identical, and thus $\bar{\theta}(\tau)\approx\theta_L(\tau)$ becomes an adequate representation of the entire temperature field. Accordingly,

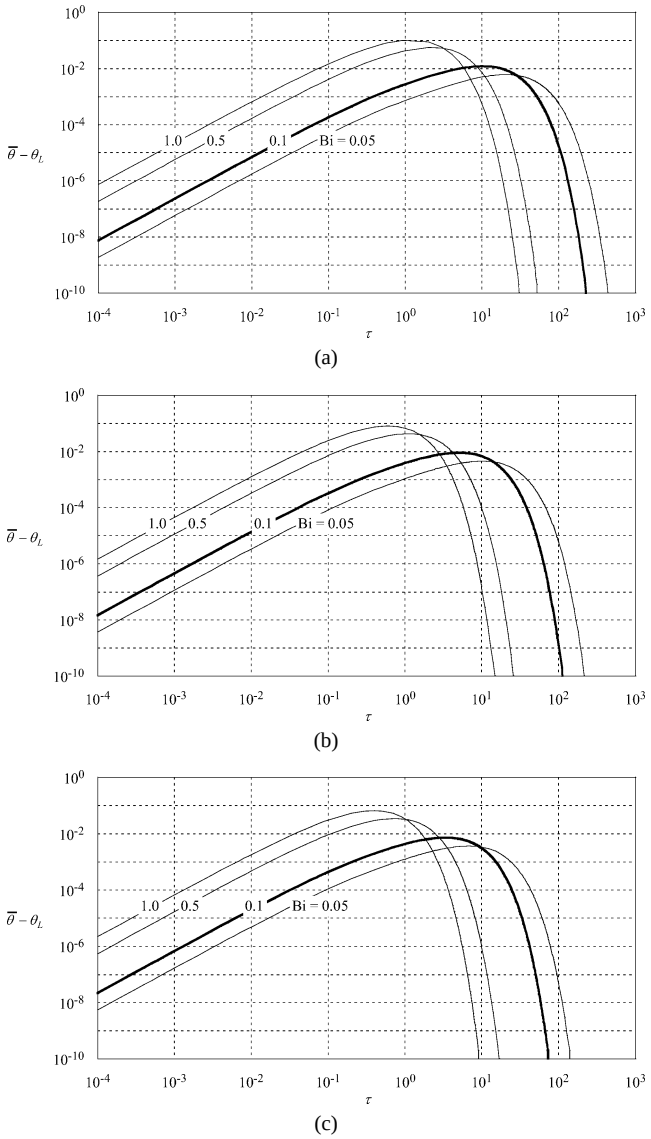

Fig. 2. Difference between lumped and exact space-mean temperatures vs. time. (a) Large plate. (b) Long cylinder. (c) Sphere.

the spatial average $\bar{\theta}$ should constitute the objective basis for studying the accuracy of the lumped solution θ_L.

The comparison between $\bar{\theta}$ and θ_L is accomplished in Fig. 2 by the simple expedient of representing the difference $\bar{\theta} - \theta_L$ versus τ, with the Biot number as a parameter. Eq. (17) has been evaluated numerically with an absolute precision better than 10^{-10}, and the scales are logarithmic for clarity. Defined in this way, the error turns out to be always positive, indicating that a lumped calculation overestimates the cooling of the body, inasmuch as the conduction resistance is neglected. The deviation $\bar{\theta} - \theta_L$ exhibits a maximum with respect to τ, which arises from the fact that both temperatures share their initial condition, Eqs. (9b) and (16b). Starting from $\tau = 0$, the error grows, but it should end at zero, since the exact and lumped solutions also share an identical asymptotic character, due to the influence of the exponential functions.

The graphical results for different *Bi* show how the generic criterion stated by Eq. (1) takes form. The classical inequality $Bi \leqslant 0.1$ approximately assures a maximum error $\bar{\theta} - \theta_L \leqslant 0.01$ for the three simple bodies in hand, i.e., that $\bar{\theta} \approx \theta_L$.

Interestingly, this latter condition is slightly more sensitive to the geometry than the traditional condition of uniformity given by Eq. (3). For $Bi = 0.1$, the maximum temperature differences in Fig. 2 are 0.0121 (slab), 0.0091 (cylinder) and 0.0073 (sphere). In contrast, more precise figures for the temperature ratio of Eq. (3) at $Bi = 0.1$ are very alike: 0.9520, 0.9518 and 0.9517, respectively. Therefore, the traditional condition is somehow hiding these differences.

6. One-term approximation of the space-mean temperature

The main feature of the lumped model solution, Eq. (10), is the exponential decay of temperature with time. An intriguing aspect of the exact solution provided by Eqs. (6) and (17) is that it parallels the same behavior, but in a rather contorted way. Due to the periodic (or almost periodic) character of the eigenfunctions, there is an infinite number of increasing eigenvalues ξ_n. Since the general term of the infinite series contains the factor $\exp(-\xi_n^2\tau)$, its magnitude decreases with n for a given τ. Therefore, an instant of time should exist at which the summation can be substituted by its first term with arbitrary precision. From that time on, Eqs. (6) and (17) reduce to

$$\theta_1(\eta, \tau) = C_1 f(\xi_1 \eta) \exp\bigl(-\xi_1^2 \tau\bigr) \tag{19}$$

$$\bar{\theta}_1(\tau) = C_1 F(\xi_1) \exp\bigl(-\xi_1^2 \tau\bigr) \tag{20}$$

The preceding simplification is of course remarkable. In fact, the above equations have been traditionally used for giving the exact solutions of unsteady cooling without resorting to the summation of a series. The Heisler–Gröber charts [5,6] are the most representative example of this widespread practice. However, it is worth to remember that Eq. (19) is only a partial solution, valid for long times. In particular, it does not satisfy the initial condition, Eq. (5b). The usual criterion for accepting the first-term approximation admits an error

$$|\theta - \theta_1| \leqslant 0.01 \tag{21}$$

for all values of the coordinate η and the parameter *Bi*. Such a condition results in a critical dimensionless time [7]:

$$\tau^* = \begin{cases} 0.24 & \text{large plate} \\ 0.21 & \text{long cylinder} \\ 0.18 & \text{sphere} \end{cases} \tag{22}$$

So that, if $\tau \geqslant \tau^*$, Eq. (19) accurately represents the exact solution, i.e., $\theta \approx \theta_1$. Furthermore, if this is satisfied at every point η, it should also apply to the spatial average. In other words, when $\tau \geqslant \tau^*$, Eq. (20) is also accurate and $\bar{\theta} \approx \bar{\theta}_1$.

Calculations between $\tau = 0$ and τ^* demand the summation of the series implied by Eqs. (6) and (17), with progressively worse convergence with decreasing time. There are however other possibilities, perhaps the most popular being based on short-time expansions of the Laplace transform [8], which is an effective method in the absence of curvature. In any case, the question has been also tackled from a more general perspective. The one-term solution is of exponential nature. Due to this unique attribute, Boussinesq designated it as a fundamental solution of unsteady heat conduction (see, for instance, the book of Kudryavtsev [9]). In the Russian literature, the one-term approximation is commonly referred to as the regular cooling, conceived as an intermediate regime between the initial condition and the final steady state. Patankar [10] independently noted the analogy of these concepts and the familiar notions of entrance and full development in forced convection theory.

7. Comparison of lumped and one-term approximations

It is clear that the similarity of both asymptotic solutions (small *Bi* and large τ) cannot be casual. Both approximations of the space-mean temperature, Eqs. (10) and (20), are exponential. Moreover, they exhibit a curious reciprocity property. The magnitude of $\bar{\theta}_1$ approximates $\bar{\theta}$ for long times and all *Bi* but never satisfies the initial condition, Eq. (16b). In contrast, θ_L is inaccurate for large *Bi*, but complies with Eq. (16b), and thus it is always exact for very short times.

The question can be elucidated by studying how the numerical value of the Biot number changes the behavior of the infinite series, i.e., the eigenvalues and constants of the series solution [11,12]. Firstly, when $Bi = 0$, the eigenconditions for ξ_n become

Large plate:

$$\xi_n \sin \xi_n = 0 \tag{23a}$$

Long cylinder:

$$\xi_n J_1(\xi_n) = 0 \tag{23b}$$

Sphere:

$$\xi_n \cos \xi_n - \sin \xi_n = 0 \tag{23c}$$

Inspection of these transcendental equations reveals that, in the three cases, the first eigenvalue is $\xi_1 = 0$, whereas $\xi_2, \xi_3, \ldots, \xi_n > 0$. Substituting thereafter for the constants C_n listed in Table 1, we immediately obtain $C_n = 0$ when $n > 1$, but C_1 becomes indeterminate. This limit can be reduced to expressions of the type $\sin \xi_1/\xi_1$ and $J_1(\xi_1)/\xi_1$, which do have a definite value at $\xi_1 = 0$. For the sake of clarity, we have left the mathematical details to an Appendix A. The final result is that C_1 equals unity when *Bi* is made arbitrarily small.

Summarizing, the limit of the constants C_n as $Bi \to 0$ can be expressed concisely as:

$$\lim_{Bi \to 0} C_n = \begin{cases} 1 & n = 1 \\ 0 & n > 1 \end{cases} \tag{24}$$

At a first glance, the discussion may appear trivial. Using Eq. (24) and $\xi_1 = 0$ in the series solution, namely, Eqs. (6) and (17), we obtain $\theta = \bar{\theta} = 1$. This reflects the obvious fact that an insulated body, $Bi = 0$, would remain forever at the initial state. Notwithstanding that, we can alternatively consider the problem in which $Bi \to 0$ without completely vanishing. Then, Eq. (24) indicates that, as *Bi* decreases, the tendency of the series to converge to the first term intensifies. Obviously, this assertion is relative. Since there is an infinity of terms with $n > 1$, its joint contribution can be of significance in spite of the implications of Eq. (24). The result will depend on the value of the time τ contained in the successive factors $\exp(-\xi_n^2 \tau)$. In conclusion, Eq. (24) may be interpreted as follows. For any *Bi* contained in $0 < Bi < \infty$, there always exists an early regime dominated by the initial condition. However, a decreasing Biot number has the effect of shortening its duration. Therefore, as $Bi \to 0$, the temperature decay accommodates sooner into an exponential behavior, or, following the Russian terminology, a regular regime.

This interpretation is confirmed by examining in further detail the traditional criterion expressed by Eqs. (21)–(22). The key element here is that these critical times cover the full range of Biot numbers and space coordinates, therefore hiding some valuable information. Table 3 reveals what occurs if we rather give the results separately with *Bi* as a parameter, considering, for instance, the flat plate. The figures have been calculated numerically by evaluating Eqs. (6) and (19) successively, with an increment of 0.01 in *Bi* and of 0.001 in τ.

The results are quite surprising. For the center and surface temperatures, the critical time exhibits a maximum with respect to *Bi*, which is located for $Bi \approx 1.5$ (This value has an uncertainty of the order of ± 0.2 due to the finite resolution in τ and *Bi*). The usual, well-known criterion logically refers to this absolute maximum, but it can be relaxed depending on the cooling conditions given by the

Table 3
Critical dimensionless time for the attainment of the regular regime in a large plate

Values of *Bi*	0.01	0.05	0.1	0.5	1	1.5	5	10	50	∞
condition at the center $\lvert\theta(0,\tau) - \theta_1(0,\tau)\rvert \leqslant 0.01$	0.00	0.00	0.06	0.20	0.23	0.24	0.22	0.20	0.18	0.17
condition at the surface $\lvert\theta(1,\tau) - \theta_1(1,\tau)\rvert \leqslant 0.01$	0.00	0.02	0.07	0.20	0.23	0.23	0.19	0.15	0.07	0.00

extent of the Biot number. When $Bi \to 0$, all critical times tend to zero, whereas they also decrease in the limit $Bi \to \infty$.

If we look for an intuitive explanation of this behavior, perhaps the following statements would be adequate. The regular regime means that the temperature variation across the coordinate η is reasonably represented by a single analytical function, $f(\xi_1\eta)$ in Eq. (19) and Table 1. In other words, since the initial condition essentially implies a discontinuity at $\eta = 1$, some time must pass before we get rid of the necessity of specifying the temperature field by an infinite series. The value of the Biot number influences this transition creating two opposing effects. If the external cooling of the body is reduced, this will favor the influence of the initial discontinuity to last longer. However, at the same time, the variation of θ with η is also reduced, thus facilitating its representation via a simple function.

For the sake of brevity, we only report detailed results for the large plate. Similar computations can be pursued for the long cylinder and the sphere, with a similar outcome. Maximum critical times with the values given in Eq. (22) always occur at the center, for $Bi \approx 2$ (cylinder) and $Bi \approx 2.3$ (sphere). Interestingly, the curvature (and the ensuing higher velocity of the transient) not only reduces the critical times, but also slightly displaces the maxima to higher Biot numbers.

As a additional result, details of the same calculation for the average temperature, Eqs. (17) and (20), are presented in Table 4 for the tree elementary geometries. A condition of validity was adopted to parallel that expressed by Eq. (21):

$$\left|\bar{\theta} - \bar{\theta}_1\right| \leqslant 0.01 \tag{21b}$$

A maximum critical time with respect to Bi is still observed, but the effects of averaging are appreciable: the value is considerably lower (0.12 vs. 0.24 for the plate) and occurs for more intense cooling, $Bi \gtrsim 6$. (The apparent plateau around the maximum is wider, preventing us to locate it with more precision in Bi than approximately ± 1.5 with the resolution used.) Figures for the cylinder and the sphere are 0.10 and 0.09, respectively. Their location is comparable to that of the plate; although the effect of the curvature is still there, its magnitude is lesser. The calculation shows that the criteria expressed by Eq. (22) can be noticeably relaxed when it is only a question of approximating the spatial average temperature. Thus, $\bar{\theta} \approx \bar{\theta}_1$ for times τ longer than a critical value τ^* given by

$$\tau^* = \begin{cases} 0.12 & \text{large plate} \\ 0.10 & \text{long cylinder} \\ 0.09 & \text{sphere} \end{cases} \tag{22b}$$

Recognizing at this point that a small Bi forces two kinds of exponential response, the next logical step is to demonstrate that both regimes are actually the same. To this end, it suffices to use again the mathematical argument that led us to Eq. (24). Since the first eigenvalue is zero for $Bi = 0$, the limit of any expression as $Bi \to 0$ is equivalent to the limit as $\xi_1 \to 0$. Applying this idea to the eigenconditions of Table 1 with $n = 1$, we could deduce that

$$\lim_{Bi\to 0} \xi_1 = (s\,Bi)^{1/2} \tag{25}$$

Similarly, considering the eigenfunctions,

$$\lim_{Bi\to 0} f(\xi_1\eta) = 1 \tag{26}$$

and the integrals $F(\xi_1)$ of Table 2:

$$\lim_{Bi\to 0} F(\xi_1) = 1 \tag{27}$$

The proof of all these propositions for the large plate, the long cylinder and the sphere is presented in Appendix A. If we combine Eqs. (24)–(27), it is straightforward to conclude that

$$\lim_{Bi\to 0} \theta_1(\eta, \tau) = \exp(-s\,Bi\,\tau) = \theta_L(\tau) \tag{28}$$

and

$$\lim_{Bi\to 0} \bar{\theta}_1(\tau) = \exp(-s\,Bi\,\tau) = \theta_L(\tau) \tag{29}$$

Accordingly, a cooling problem with a vanishingly small Biot number may be conceived as the limit at which the regular regime extends down to an arbitrarily short time, and, as a consequence, its validity encompasses the whole process. In other words, the one-term approximation is compelled to satisfy the initial condition; such a circumstance is what we usually call a lumped solution.

It is equally noteworthy that the transition manifests itself by a dramatic simplification of the geometry. As the Biot number decreases, the time constant of Eqs. (19)–(20) changes to that of Eq. (10). The complicated influence of geometric shape, as expressed by the different eigenconditions in Table 1, reduces to the parameter s, i.e., to the volume-to-area ratio, by virtue of Eq. (25). Fig. 3 represents this perspective of the lumped approximation. The exact values of ξ_1 are compared with the result of Eq. (25) for the three one-dimensional bodies, confirming that the limit is attained in the vicinity of $Bi = 0.1$. Therefore, we have arrived at a further formulation of the criterion of validity that is basically equivalent to those previously given. However, an important difference should be noted: the determination of a

Table 4
Critical dimensionless time for the validity of the one-term approximation of the average temperature, $|\bar{\theta}(\tau) - \bar{\theta}_1(\tau)| \leqslant 0.01$

Values of Bi	0.01	0.05	0.1	0.5	1	1.5	5	10	50	∞
Large plate	0.00	0.00	0.00	0.00	0.02	0.07	0.12	0.12	0.10	0.10
Long cylinder	0.00	0.00	0.00	0.00	0.02	0.06	0.10	0.10	0.09	0.09
Sphere	0.00	0.00	0.00	0.00	0.01	0.04	0.08	0.08	0.07	0.07

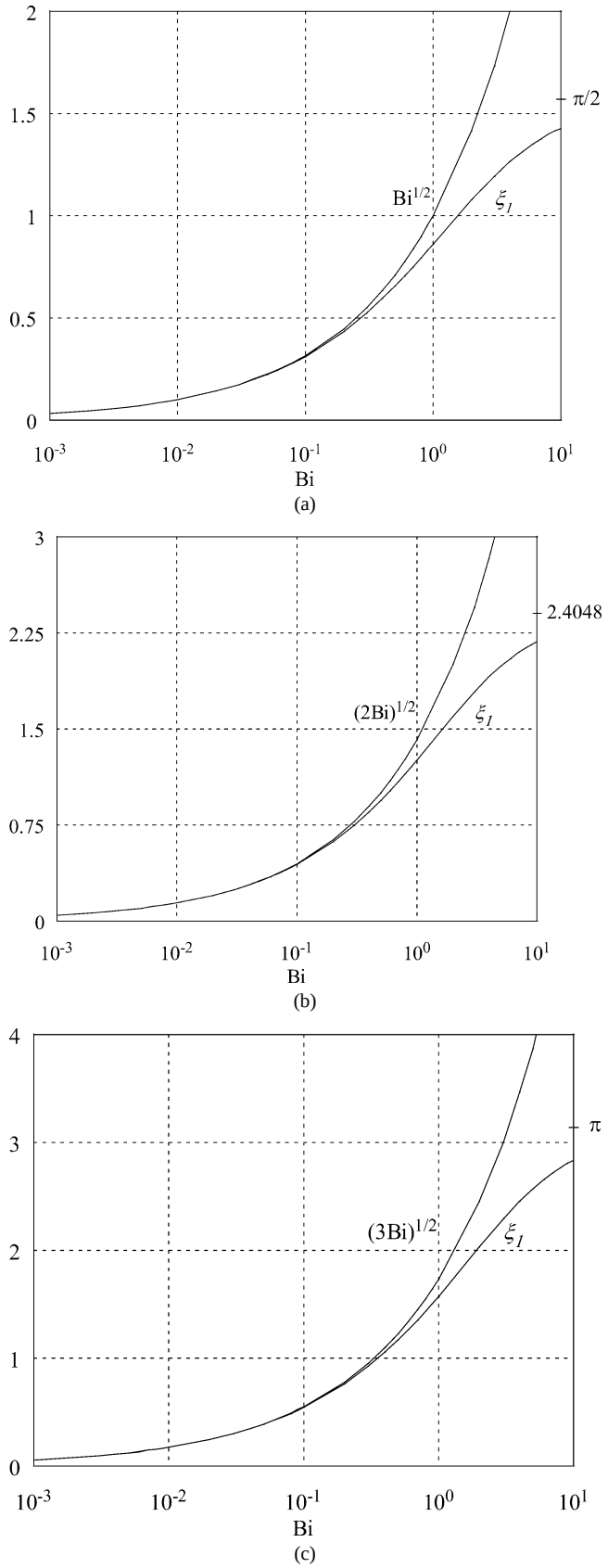

Fig. 3. Variation of the first eigenvalue (exact and lumped limit) with the Biot number. (a) Large plate. (b) Long cylinder. (c) Sphere.

acceptable maximum Biot number can now proceed without the need of an iterative procedure.

8. Conclusions and perspective

In this paper, we have examined the lumped model of unsteady heat conduction driven by convective cooling. Using as a case-study the exact temperature solutions for the three elementary, one-dimensional geometries, we have demonstrated that

(1) The traditional condition of uniformity for a lumped transient, Eq. (3), can be replaced by a maximum difference between the lumped temperature solution θ_L and the exact space-mean temperature $\bar{\theta}$. This expresses the intuitive fact that a temperature profile approximately uniform equals its average, and may serve to deduce an alternative criterion of validity for the lumped model θ_L, as displayed in Fig. 2. This criterion is more sensitive to the geometry than the usual one.
(2) The lumped solution, Eq. (10), and the one-term approximations, Eqs. (19) and (20), exhibit a reciprocity relationship. The former is the limit as $Bi \to 0$ of the general infinite series solution, whereas the latter represent the long-term solution, valid for times τ greater than an arbitrary critical value τ^*. The transition $Bi \to 0$ is equivalent to $\tau^* \to 0$, so that it may be imagined as the regime which connects the exponential lumped behavior with the exponential one-term approximation.
(3) A further method for deriving the criterion of validity can be based on the limiting behavior of the first eigenvalue ξ_1, as exemplified in Fig. 3. Although the condition is far less intuitive than the classical one, the procedure has a significant advantage: the limit value of the Biot number is deduced without resorting to an iteration.

Needless to say, all these analyses can be extended to more complex situations, as long as an infinite series solution is available. This comprises two- and three-dimensional bodies whose temperature θ is found by the method of separation of variables in the appropriate coordinate systems. It should be noted that a condition imposed on the spatial average $\bar{\theta}$ can be very useful when the location of extreme temperatures is not known a priori. In this respect, it may be said that the criteria developed in this paper are more general than those based on the customary condition expressed by Eq. (3).

On the other hand, a kind of multidimensional problems exist that could be directly handled by the methods considered in this study. The product of several series in the form of Eq. (6) and Table 1 is known to represent the nondimensional temperature field in simple geometries, such as a rectangular infinite beam or a finite cylinder. Any of the conditions considered here (including the traditional one) can be simply

combined to ascertain the accuracy of the lumped assumption in these geometries.

Acknowledgements

This work has been partially supported by the Secretary of the Council of CIRCE Foundation, University of Zaragoza. The authors gratefully acknowledge many useful suggestions and comments made by the reviewers of the original manuscript.

Appendix A. Mathematical proof of the limits as $Bi \to 0$

To demonstrate the limiting behavior of the constants, eigenvalues, eigenfunctions and integrals expressed in Eqs. (24)–(27) we need these two lemmas:

$$\lim_{a\to 0} \frac{\sin a}{a} = 1 \tag{A.1}$$

$$\lim_{a\to 0} \frac{J_1(a)}{a} = \frac{1}{2} \tag{A.2}$$

The first is a well-know result. The second can be easily deduced by applying L'Hôpital's theorem:

$$\begin{aligned}\lim_{a\to 0} \frac{J_1(a)}{a} &= \lim_{a\to 0} \frac{J_0(a) - \frac{J_1(a)}{a}}{1} \\ &= \lim_{a\to 0} J_0(a) - \lim_{a\to 0} \frac{J_1(a)}{a} \\ &= 1 - \lim_{a\to 0} \frac{J_1(a)}{a}\end{aligned} \tag{A.3}$$

where the rules of differentiation of Bessel functions have been used. Eq. (A.2) follows immediately from Eq. (A.3).

The limit of C_1 in Eq. (24) is found by substituting the condition $Bi \to 0$ by its equivalent $\xi_1 \to 0$. Using the formulae of Table 1 with $n = 1$, we obtain for the large plate:

$$\begin{aligned}\lim_{Bi\to 0} C_1 = \lim_{\xi_1\to 0} C_1 &= \lim_{\xi_1\to 0} \frac{2\sin\xi_1}{\xi_1 + \sin\xi_1\cos\xi_1} \\ &= \lim_{\xi_1\to 0} \frac{2}{\frac{\xi_1}{\sin\xi_1} + \cos\xi_1} = \frac{2}{1+1} = 1\end{aligned} \tag{A.4a}$$

Similarly, for the long cylinder:

$$\begin{aligned}\lim_{Bi\to 0} C_1 &= \lim_{\xi_1\to 0} \frac{2J_1(\xi_1)}{\xi_1(J_0^2(\xi_1) + J_1^2(\xi_1))} \\ &= \lim_{\xi_1\to 0} \frac{2}{\frac{\xi_1}{J_1(\xi_1)}(J_0^2(\xi_1) + J_1^2(\xi_1))} \\ &= \frac{2}{2\cdot 1} = 1\end{aligned} \tag{A.4b}$$

In the case of the sphere, we have to resort a second time to L'Hôpital's theorem:

$$\begin{aligned}\lim_{Bi\to 0} C_1 &= \lim_{\xi_1\to 0} \frac{2(\sin\xi_1 - \xi_1\cos\xi_1)}{\xi_1 - \sin\xi_1\cos\xi_1} \\ &= \lim_{\xi_1\to 0} \frac{2(\cos\xi_1 - \cos\xi_1 + \xi_1\sin\xi_1)}{1 + \sin^2\xi_1 - \cos^2\xi_1} \\ &= \lim_{\xi_1\to 0} \frac{2\xi_1\sin\xi_1}{2\sin^2\xi_1} = \lim_{\xi_1\to 0} \frac{\xi_1}{\sin\xi_1} = 1\end{aligned} \tag{A.4c}$$

Next, to find the limit of the first eigenvalue, Eq. (25), the three eigenconditions for ξ_1 in Table 1 are written in this manner:

Large plate:

$$Bi = \xi_1 \frac{\sin\xi_1}{\cos\xi_1} \tag{A.5a}$$

Long cylinder:

$$Bi = \xi_1 \frac{J_1(\xi_1)}{J_0(\xi_1)} \tag{A.5b}$$

Sphere:

$$Bi = \frac{\sin\xi_1 - \xi_1\cos\xi_1}{\sin\xi_1} \tag{A.5c}$$

Dividing by ξ_1^2 and taking the limit, we easily deduce for the large slab and the long cylinder, respectively:

$$\lim_{Bi\to 0} \frac{Bi}{\xi_1^2} = \lim_{\xi_1\to 0} \frac{Bi}{\xi_1^2} = \lim_{\xi_1\to 0} \frac{\sin\xi_1}{\xi_1}\frac{1}{\cos\xi_1} = 1\cdot 1 = 1 \tag{A.6a}$$

$$\begin{aligned}\lim_{Bi\to 0} \frac{Bi}{\xi_1^2} &= \lim_{\xi_1\to 0} \frac{Bi}{\xi_1^2} = \lim_{\xi_1\to 0} \frac{J_1(\xi_1)}{\xi_1}\frac{1}{J_0(\xi_1)} \\ &= \frac{1}{2}\cdot 1 = \frac{1}{2}\end{aligned} \tag{A.6b}$$

Once again, the eigenvalue of the sphere demands a special treatment, resulting in:

$$\begin{aligned}\lim_{Bi\to 0} \frac{Bi}{\xi_1^2} &= \lim_{\xi_1\to 0} \frac{\sin\xi_1 - \xi_1\cos\xi_1}{\xi_1^2\sin\xi_1} \\ &= \lim_{\xi_1\to 0} \frac{\cos\xi_1 - \cos\xi_1 + \xi_1\sin\xi_1}{2\xi_1\sin\xi_1 + \xi_1^2\cos\xi_1} \\ &= \lim_{\xi_1\to 0} \frac{\sin\xi_1}{2\sin\xi_1 + \xi_1\cos\xi_1} \\ &= \lim_{\xi_1\to 0} \frac{1}{2 + \frac{\xi_1}{\sin\xi_1}\cos\xi_1} = \frac{1}{2+1\cdot 1} = \frac{1}{3}\end{aligned} \tag{A.6c}$$

The limit of the first eigenfunctions in Table 1, Eq. (26), directly follows from elementary considerations and Eqs. (A.1) and (A.2). Aside from a new application of L'Hôpital's theorem in the spherical case, the same argument holds for Eq. (27) concerning the integrals $F(\xi_1)$ of Table 2.

References

[1] V. Arpaci, Conduction Heat Transfer, Addison-Wesley, Reading, MA, 1966.
[2] A.V. Luikov, Analytical Heat Diffusion Theory, Academic, New York, 1968.

[3] R. Courant, D. Hilbert, Methods of Mathematical Physics, Interscience, New York, 1953.

[4] M.N. Ozisik, Heat Conduction, Wiley, New York, 1980, Chapter 9.

[5] M.P. Heisler, Temperature charts for induction and constant temperature heating, Trans. ASME 69 (1947) 227–236.

[6] H. Gröber, S. Erk, U. Grigull, Fundamentals of Heat Transfer, McGraw-Hill, New York, 1961, Chapter 3.

[7] U. Grigull, H. Sandner, Heat Conduction, Springer/Hemisphere, New York, 1984, Chapter 6.

[8] M.N. Ozisik, Heat Conduction, Wiley, New York, 1980, Chapter 7.

[9] Y.V. Kudryavtsev, Unsteady State Heat Transfer, Iliffe Books, London, 1966, Chapter 1.

[10] S.V. Patankar, The concept of a developed regime in unsteady heat conduction, in: Studies in Heat Transfer, Hemisphere, New York, 1979, pp. 419–431.

[11] V. Isachenko, V. Osipova, A. Sukomel, Heat Transfer, MIR, Moscow, 1977, Chapter 3.

[12] J. Fourier, The Analytical Theory of Heat, Dover, New York, 1955, Chapter V.